DEUTSCHES ELEKTRONEN-SYNCHROTRON DESY

DESY SR-79/27
October 1979

3p - 3d INTERSHELL INTERACTION IN Cr

by

J. Barth, F. Gerken, K.L.I. Kobayashi, J. H. Weaver and B. Sonntag
II. Institut für Experimentalphysik der Universität Hamburg
and
Deutsches Elektronen-Synchrotron DESY, Hamburg

NOTKESTRASSE 85 · 2 HAMBURG 52

To be sure that your preprints are promptly included in the
HIGH ENERGY PHYSICS INDEX ,
send them to the following address (if possible by air mail) :

DESY
Bibliothek
Notkestrasse 85
2 Hamburg 52
Germany

DESY SR-79/27
October 1979

3p - 3d Intershell Interaction in Cr

J. Barth, F. Gerken, K.L.I. Kobayashi[+], J.H. Weaver[*] and

B. Sonntag

II. Institut für Experimentalphysik Hamburg and Deutsches

Elektronensynchrotron DESY, Hamburg, Germany

The photoemission of Cr films deposited under UHV conditions has been investigated in the photon energy range from 30 eV to 230 eV. The 3p - 3d intershell interaction gives rise to a strong maximum in the 3d partial yield above the 3p threshold.

+) Central Research Laboratory, Hitachi, Ltd.
Kokubunji, Tokyo 185, Japan

*) Synchrotron Radiation Center, University of Wisconsin,
Stoughton, Wisconsin 53589, United States of America

The interference between the $3p^6\ 3d^N \rightarrow 3p^5\ 3d^{N+1}$ and $3p^6\ 3d^N \rightarrow 3p^6\ 3d^{N-1}\ \varepsilon f$ transitions coupled via the super-Coster-Kronig transition $3p^5\ 3d^{N+1} \rightarrow 3p^6\ 3d^{N-1}\ \varepsilon f$ has been invoked as an explanation of the 3p absorption spectra of the atomic and solid 3d transition metals (Dietz et al. 1974, Davis and Feldkamp 1976, 1978, Bruhn et al. 1979, 1978). For Mn to Cu theoretical calculations (Davis and Feldkamp 1976, 1978) and the agreement between the spectra of the free atoms and those of the corresponding metals (Bruhn et al. 1979, 1978) support this interpretation. For Cr however the 3p spectra of the metal and the free atoms are completely different (Bruhn et al. 1979, Mansfield 1977) indicating a breakdown of the atomic model. In order to assess the importance of the 3p - 3d intershell interaction, the relative 3p and 3d subshell cross-sections of Cr metal have been determined.

The Cr films, evaporated under UHV conditions (base pressure of the system $1 \cdot 10^{-10}$ Torr, pressure during evaporation $5 \cdot 10^{-9}$ Torr) onto Si substrates were illuminated by the synchrotron radiation of the storage ring DORIS monochromatized by the Flipper monochromator (Eberhardt 1978, Eberhardt et al. 1978). The cleanliness of the samples was checked by Auger spectroscopy. The photoelectrons were analyzed by a double path cylindrical mirror analyzer whose axis was perpendicular to the incoming photon beam and tilted by 45° against the plane of the elctric vector of the radiation. The samples were illuminated under 45° by s-polarized light. In respect to the axis of the cylindrical analyzer, the collection geometry corresponds to averaging the emission over all azimuthal angles and polar angles between 36° and 48°. Details of the experimental arrangement are given by Eberhardt 1978, Eberhardt et al. 1978, and Kalkoffen 1978. The results obtained at DORIS were confirmed by measurements performed with synchrotron radiation of the storage ring TANTALUS I monochromatized by a GRASSHOPPER monochromator (Brown et al. 1978). The experimental set-up was similar to the one used at DORIS. The Cr films were evaporated under UHV conditions (base pressure of the system $5 \cdot 10^{-11}$ Torr, pressure during evaporation $5 \cdot 10^{-10}$ Torr) onto stainless steel substrates.

Energy distribution curves (EDC's) for several photon energies are presented in Fig. 1. These EDC's taken with an overall resolution of 0.45 eV are normalized to the photon flux impinging on the sample. Photoemission from the Cr valence band (V), mainly originating from the Cr 3d states, gives rise to an approximately 4 eV wide band below the Fermi level (E_F). This band peaks between 1.5 eV and 2 eV below E_F. Two shoulders are clearly discernible at 0.5 eV and 3.5 eV binding energy. For comparison we have included calculated densities of states (Prince and Waber 1971). The experimental and theoretical results agree in respect to the triple structure and the overall width. The maximum at 6 eV binding energy having a weak counterpart in the calculated density of states may be related to a similar peak detected for Ni which goes through a resonance at the 3p threshold (Guillot et al. 1977). In contrast to the 6 eV peak in Ni, the Cr peak does not show a pronounced enhancement when scanning the photon energy through the 3p threshold. A detailed analysis of the energy dependence of the peak intensity is very difficult, because of the overlapping MVV Auger transitions. The MVV Auger edge clearly shows up between 4 eV and 8 eV below E_F for 46 eV photon energy. The Auger edge shifts towards higher binding energies with increasing photon energy. For photon

energies below 46 eV the Auger electrons are hard to disentangle from the valence band photoelectrons. As can be seen qualitatively from Fig. 1, the intensity of the valence band emission goes through a marked minimum at $h\omega \sim 42$ eV. For a more detailed analysis the relative valence band, 3p and 3s subshell cross-sections shown in Fig. 2 have been extracted from a series of EDC's measured at photon energies between 30 eV and 230 eV. Before determining the area of the corresponding photoemission peaks, the EDC's were corrected for the spectral output of the monochromator, the variation of the current in the storage ring, the transmission and collection efficiency of the cylindrical analyzer. The collection efficiency was assumed to be proportional to the ratio of the pass energy E_p to the kinetic energy E_k (Palmberg 1974). This is in agreement with the intensity variation of a photoemission line with pass energy determined experimentally for our set-up. For the valence band cross-section all electrons with binding energies between E_F and ~ 8 eV have been taken into account. Secondary electron background determined by interpolation (see e.g. Fig. 1) has been subtracted. For photon energies below 90 eV the 3p photoemission peak merges into the background of low energy scattered electrons. Therefore, in this range the 3p subshell cross-section has been estimated from the number of MVV Auger electrons. For comparison the subshell cross-sections calculated by McGuire 1970 are also given. The relative spectral dependence of the $3p \rightarrow \varepsilon d$, εs, and $3s \rightarrow \varepsilon p$ subshell cross-sections are in agreement with theoretical subshell photoionization cross-sections for atomic Cr (McGuire 1970, Kelly and Ron 1972). The 3p subshell cross-section shows the maximum at threshold, the Cooper minimum and the subsequent rise towards higher photon energies. The valence band cross-section deviates markedly from the spectral behavior predicted for the 3d subshell cross-section (McGuire 1970, Kelly and Ron 1972). The minimum at 42 eV

and the prominent double maximum peaking at 52 eV and at 70 eV have no counterparts in the theoretical curves which show a smoothly decreasing 3d cross-section in the energy range under consideration. The 3d subshell cross-section for metallic Ni shows a similar double peak above the 3p threshold. The energy dependence of the photoemission intensity of the Ni d-band obtained in the same way as for Cr is included in Fig. 2. Barth et al. (1979) demonstrated for Ni that the shape of the 3d subshell yield close to the 3p threshold (66 eV) strongly varies for different parts of the d-band and the satellite. In contrast the broad maximum centered at 100 eV photon energy stays the same for all parts of the d-band. The sum of the experimental 3d and 3p subshell cross-sections, the partial yield spectrum obtained for 2 eV kinetic energy electrons and the absorption spectrum (Sonntag et al., 1969) are presented in Fig. 3. In summing the subshell cross-sections, the small 3s contribution has been neglected. From the M_1VV Auger intensity it has been estimated to be less than half the 3p subshell cross-section in the photon energy range 75 eV - 140 eV. The three spectra shown in Fig. 3 have been adjusted below the 3p threshold. They all show a ~ 20 eV wide, structured maximum above the 3p threshold. The yield spectrum is in fair agreement with the absorption spectrum. The most striking result is the low amplitude of the maxima of the sum of the 3p and 3d subshell cross-sections. Above 80 eV there is reasonable agreement between the sum of the 3p and 3d subshell cross-sections and the absorption. Since the number of low energy scattered electrons per primary electron increases with the energy of the primary electron, it is no surprise that the yield overshoots the other spectra at higher photon energies. The low energy maximum centered at 52 eV for the subshell sum spectrum splits in two peaks (49 eV and 55 eV) in the yield and the absorption spectrum. The high

energy maximum in the subshell spectrum has its counterpart in the broad shoulder centered at 70 eV in the yield spectrum. There is no corresponding maximum in the absorption spectrum. Several possible explanations are discussed in the following.

The angular distribution of photoelectrons emitted from free atoms is given by $1 + \beta P_2(\cos\ )$, where β is the angle between the electric field of the radiation and the direction of the outgoing electron. Integrating this expression over all angles accepted by the cylindrical analyzer results in $1 + \beta' 0.08$. Even in the case of extreme variations of the atomic asymmetry parameter β with photon energy, this effect cannot account for the strong modulation observed for the Cr 3d yield between 40 eV and 100 eV.

Solid state effects can give rise to modulations of subshell cross-sections extending far above threshold. These modulations have been observed in angle resolved (Tong and Stoner 1978) and angle integrated (Petersen and Kunz 1975, Margaritondo and Stoffel 1979) photoemission measurements. The collection geometry, the polycrystalline nature of the Cr samples and the existence of the maximum in the partial yield spectrum renders an explanation in terms of photoelectron diffraction (Tong and Stoner 1978) very improbable. Such strong modulations of the 3d subshell absorption cross-section due to solid state effects are also not very likely. Presently, a definite answer cannot be given, because there are no band calculations for Cr and Ni extending so far above E_F which would allow the calculation of an

absorption spectrum taking matrix element effects into account. In a simple EXAFS-like approach for photon energies above 100 eV we expect the 3d subshell cross-section of Cr and Ni to show similar modulations because the nearest neighbor distance (2.5 Å) is the same for both metals and the phase shifts should not vary very much from Cr to Ni. This is borne out e.g. by 1s EXAFS spectra of both metals (Rabe et al. 1979). Closer to threshold the different crystal structures (Cr bcc, Ni fcc) give rise to deviations. For Cr and Ni the maxima show up within 30 eV above the 3p threshold. There are no marked maxima for higher photon energies. This indicates that the 3p - 3d intershell interaction is responsible for the enhanced 3d subshell cross-sections above the 3p threshold. The formation of a d-like resonance state due to the influence of the neighboring atoms may be an additional ingredient.

The discrepancies between the three spectra shown in Fig. 3 can be accounted for by assuming that not all processes contributing to the absorption are comprised in the experimental subshell spectrum. For clarification of this point the absorption and decay processes resulting in the emission of primary photoelectrons are schematically depicted in Fig. 4. Because of the local character of the 3p and 3d states and the strength of the 3p - 3d interaction, an atomic approach is justified. Column I of Fig. 4 gives the $3p \rightarrow \varepsilon s$, εd continuum transitions, the only transitions taken into account by McGuire's (1970) 3p subshell cross-section.

The excited $3p^5\ 3d^5\varepsilon_1 l_1$ states dominantly decay via super-Coster-Kronig transitions into $3p^6\ 3d^3\varepsilon_1 l_1\ \ \varepsilon_2 l_2$ (column II Fig. 4). The 3p subshell cross-section given in Fig. 2 has been obtained by determining the number of photoelectrons ($\varepsilon_1 l_1$) above 90 eV and estimating the number of Auger electrons ($\varepsilon_2 l_2$) below 90 eV. The energy of the excited $Cr^+\ 3p^5\ 3d^5$ ion can be shared in different ways by the $Cr^{++}\ 3p^6\ 3d^3$ ion and the Auger electron. This may give rise to Auger satellites and add to the width of the energy distribution of the Auger electrons. The reasonable agreement between the experimental and theoretical curves indicates that except for those close to threshold the 3p → εs, εd continuum transitions are not strongly coupled to other channels. For simplicity the delocalized 4s electrons have been omitted.

The main contribution to the absorption close to the 3p threshold stems from the 3p → 3d transitions (Dietz et al. 1974, Davis and Feldkamp 1976, 1978, Bruhn et al. 1979, 1978, McGuire 1972) which have not been incorporated in the calculated subshell cross-sections (McGuire 1970). These transitions are depicted in column IV of Fig. 5. The interaction of the partly filled $3d^6$ shell with the $3p^5$ shell results in a multiplet splitting of ∿ 20 eV (Davis and Feldkamp 1979) and raises part of the oscillator strength above the lowest ionization limit. The "super-Coster-Kronig" decay $3p^5\ 3d^6 \rightarrow 3p^6\ 3d^4\ \varepsilon_5 l_5$ results in the emission of high energy electrons ($\varepsilon_5 l_5$). By the quotation marks we want to point out that the super-Coster-Kronig process is indistinguishable from the

autoionization process which leads to the same final state. The fact that the $3p^6\ 3d^4\ \varepsilon_5 l_5$ states can also be reached by direct excitation of a 3d electron gives rise to interference between the two excitation channels (Dietz et al. 1974, Davis and Feldkamp 1976 and 1978, Bruhn et al. 1979 and 1978). The 3d subshell cross-section given in Fig. 2 has been obtained by the determination of the intensity of the $\varepsilon_5 l_5$ electrons (Column V of Fig. 4). There are further decay channels for the excited $3p^5\ 3d^6$ state. The channels we consider most important are shown in Fig. 4. Column III gives the final state reached by an Auger decay accompanied by a shake-up process. Here $n_3 l_3$ stands for a bound electron. These states, which are also accessible by direct excitation of two d electrons, have been invoked as an explanation for the strong resonances in the valence band photoemission spectra of Cu and Ni (Iwan et al. 1979, Wolff 1979). The autoionization process $3p^5\ 3d^6 \rightarrow 3p^5\ 3d^5\ \varepsilon_6 l_6$ has been proposed by Dehmer et al. (1971). This autoionization process is followed by a super-Coster-Kronig transition resulting in two continuum electrons ($\varepsilon_6 l_6$, $\varepsilon_7 l_7$). It is obvious that these channels are not fully covered by our measurements. Therefore, a considerable fraction of the $3p^6\ 3d^5 \rightarrow 3p^5\ 3d^6$ oscillator strength is missing in the sum of the 3p and 3d subshell cross-sections presented in Fig. 3. According to our results the 3d subshell cross section only comprises approximately 25% of the 3p → 3d oscillator strength. This is similar to the finding of Lenth et al. (1978) for the 4d → 4f transitions in rare earth compounds. The large discrepancy between the (3p + 3d) subshell cross-section and the absorption given in Fig. 4 indicates that the decay

channels discussed above are not negligible compared to the $3p^5\ 3d^6 \rightarrow 3p^6\ 3d^4\ {}_5l_5$ super-Coster-Kronig decay.

In summarizing we state:

i) There is a strong 3p - 3d intershell interaction.

ii) The maxima in the 3d subshell cross-section above the 3p threshold originate from the $3p^6\ 3d^5 \rightarrow 3p^5\ 3d^6$ excitations.

iii) Due to the contribution of different decay mechanisms, the oscillator strength of the $3p^6\ 3d^5 \rightarrow 3p^5\ 3d^6$ transitions present in the absorption spectrum is not fully covered by the sum of the 3p and 3d subshell cross-sections.

The authors want to thank M. Iwan, C. Kunz and H.W. Wolff for many stimulating discussions.

References

J. Barth, G. Kalkoffen and C. Kunz, Phys. Lett. A (in press)

R. Bruhn, B. Sonntag and H.W. Wolff 1978, Phys. Lett. 69A, 9

R. Bruhn, B. Sonntag and H.W. Wolff 1979, J. Phys. B 12, 203

R. Bruhn, B. Sonntag and H.W. Wolff 1979 to be published

F.C. Brown, R.Z.Bachrach and N. Lien 1978, Nucl. Instr. and Methods 152, 73

L.C. Davis and L.A. Feldkamp 1976, Solid St. Comm. 19, 413

L.C. Davis and L.A. Feldkamp 1978, Phys. Rev. A 17, 2012

L.C. Davis and L.A. Feldkamp 1979, private communication

I.L. Dehmer, A.F. Starace, U. Fano, I. Sugar and I.W. Cooper 1971, Phys. Rev. Lett. 26, 1521

R.E. Dietz, E.G. McRae, Y. Yafet and C.W. Caldwell 1974, Phys. Rev. Lett. 33, 1372

W. Eberhardt 1978, Thesis University of Hamburg

W. Eberhardt, G. Kalkoffen and C. Kunz 1978, Nucl. Instr. and Methods 152, 81

W. Gudat and C. Kunz 1972, Phys. Rev. Lett. 29, 169

C. Guillot, Y. Ballu, J. Paigné, I. Lecante, K.-P. Jain, P. Thiry, R. Pinchaus, Y. Petroff and L.M. Falicov 1977, Phys. Rev. Lett. 25, 1632

M. Iwan, F.J. Himpsel and D.E. Eastman 1979, Phys. Rev. Lett. (in press)

G. Kalkoffen 1978, Thesis University of Hamburg

H.P. Kelly and A. Ron 1972, Phys. Rev. A5, 168

W. Lenth, F. Lutz, J. Barth, G. Kalkoffen and C. Kunz 1978, Phys. Rev. Lett. 41, 1185

M.W.D. Mansfield 1977, Proc. Roy. Soc. Lond. A358, 253

G. Margaritondo and N.G. Stoffel 1979, Phys. Rev. Lett. 42, 1567

E.I. McGuire 1970, Sandia Laboratories Research Report SC-RR-70-721

E.I. McGuire 1972, J.Phys. Chem. Solids 33, 577

P.W. Palmberg 1974, J.Electron. Spectr. and Related Phenomena 5, 691

H. Petersen and C. Kunz 1975, Phys. Rev. Lett. 35, 863

M.Y. Prince and I.T. Waber 1971 in Electronic Density of States, ed. L.H. Bennett, NBS Spec. Publ. 323, 222

P. Rabe, G. Tolkiehn and A. Werner 1979, private communication

B. Sonntag, R. Haensel and C. Kunz 1969, Solid St. Commun. 7, 597

S.Y. Tong and N. Stoner 1978, J. Phys. C 11, 3511

H.W. Wolff 1979, Thesis University of Hamburg

Figure Captions

Fig. 1 Electron energy distribution curves for solid Cr normalized to the number of photons impinging on the sample. The dashed line gives the estimated background of scattered electrons. The calculated density of valence band states (Prince and Waber 1971) is shown by the dotted curve.

Fig. 2 3d, 3p and 3s subshell cross-sections for solid Cr. The solid curves provide reasonable fits to the data points; ● for 3d; ○ for 3p, obtained directly; ◇ for 3p, obtained via the Auger yield; x for 3s. The dashed and dashed-dotted curves present the 3d (---), 3p (-·-) and 3s (-···-) subshell cross-sections calculated by McGuire 1970. The insert gives the energy dependence of the electrons emitted from the Ni d-band.

Fig. 3 Experimental absorption cross-section, partial yield of zero kinetic energy electrons and sum of the 3p and 3d subshell cross-sections for solid Cr.

Fig. 4 Schematic picture of the important excitation and decay processes above the 3p threshold of solid Cr.

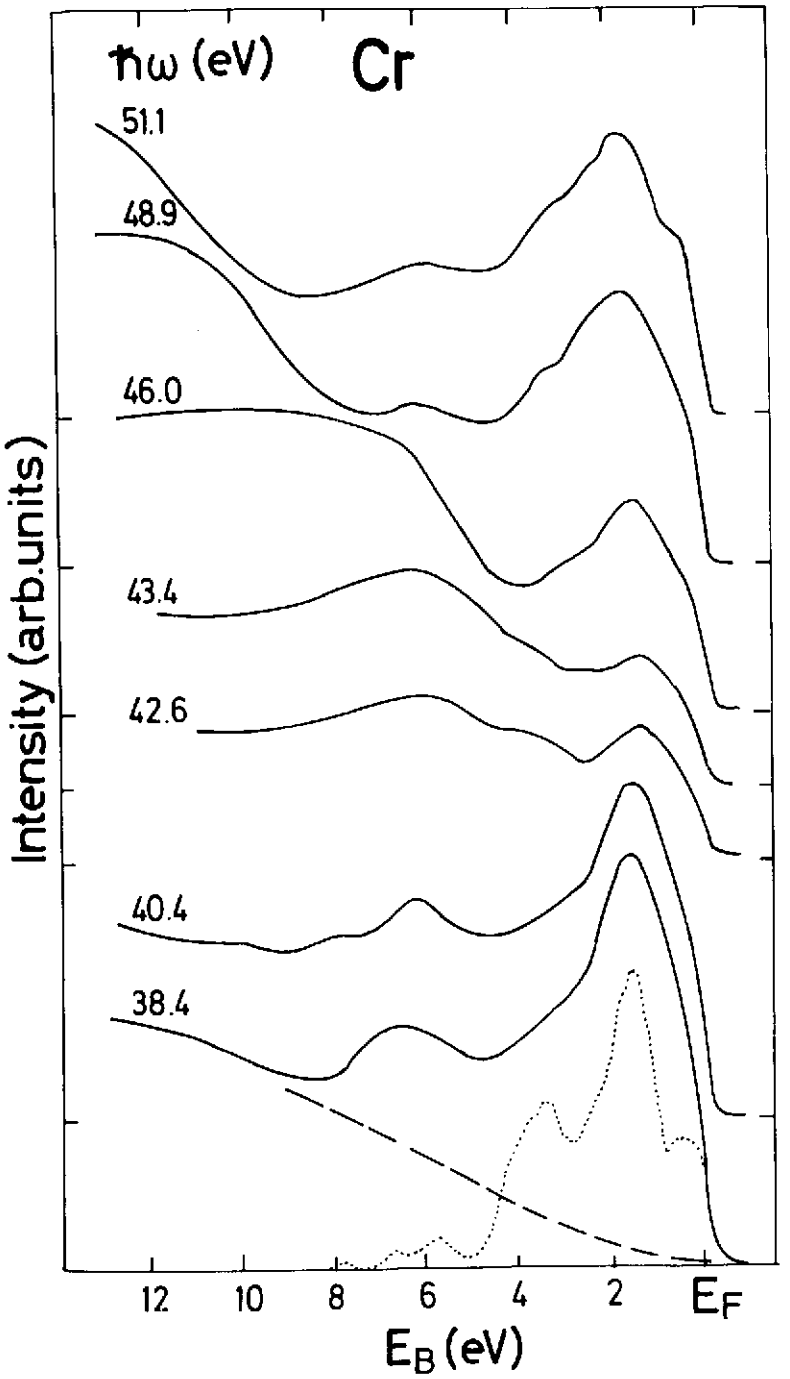
ħω (eV)
Cr
51.1
48.9
46.0
43.4
42.6
40.4
38.4
Intensity (arb.units)
12
10
8
6
4
2
E_F
E_B (eV)

Fig. 1

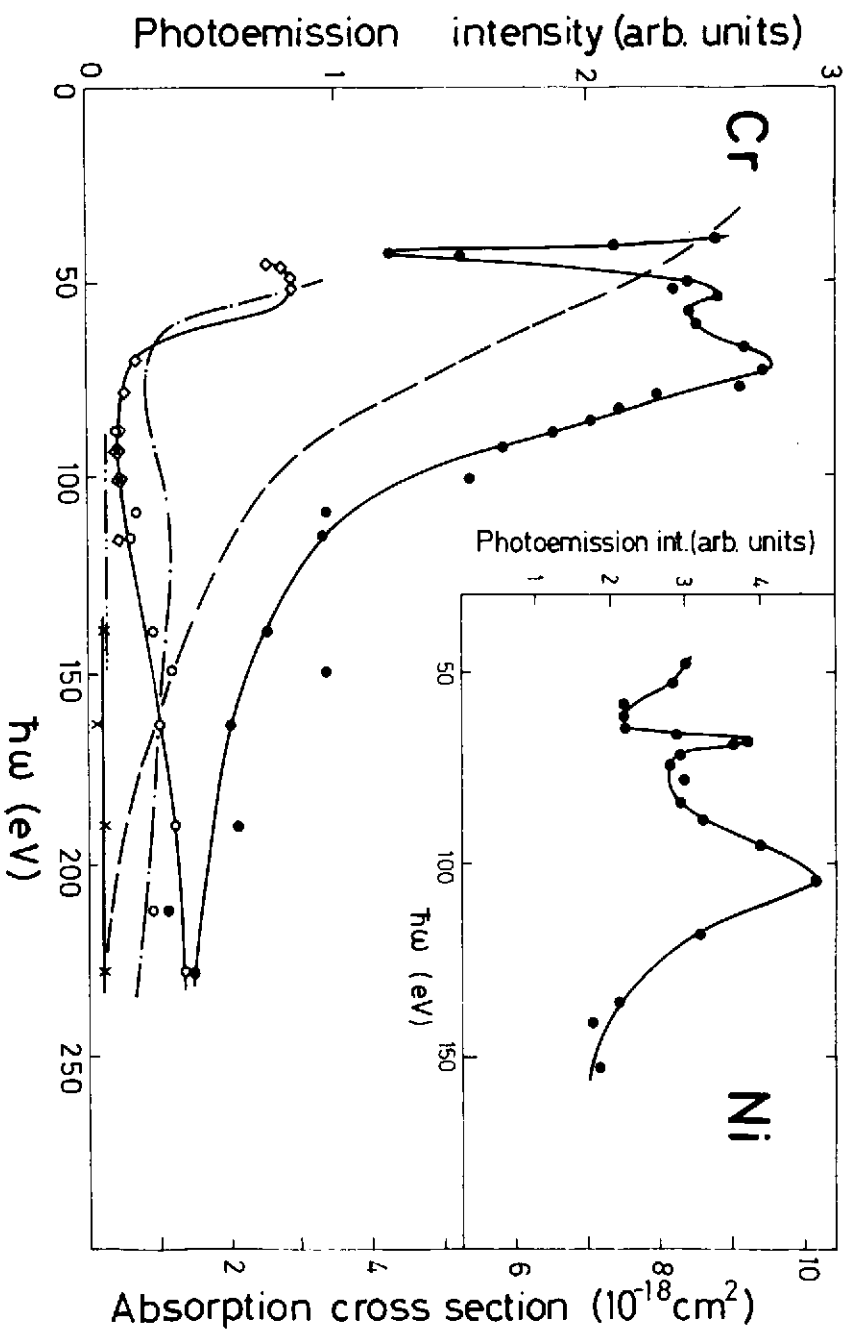
Photoemission intensity (arb. units)
Cr
ħω (eV)
Photoemission int.(arb. units)
ħω (eV)
Ni
Absorption cross section (10^-18 cm^2)

Fig. 2

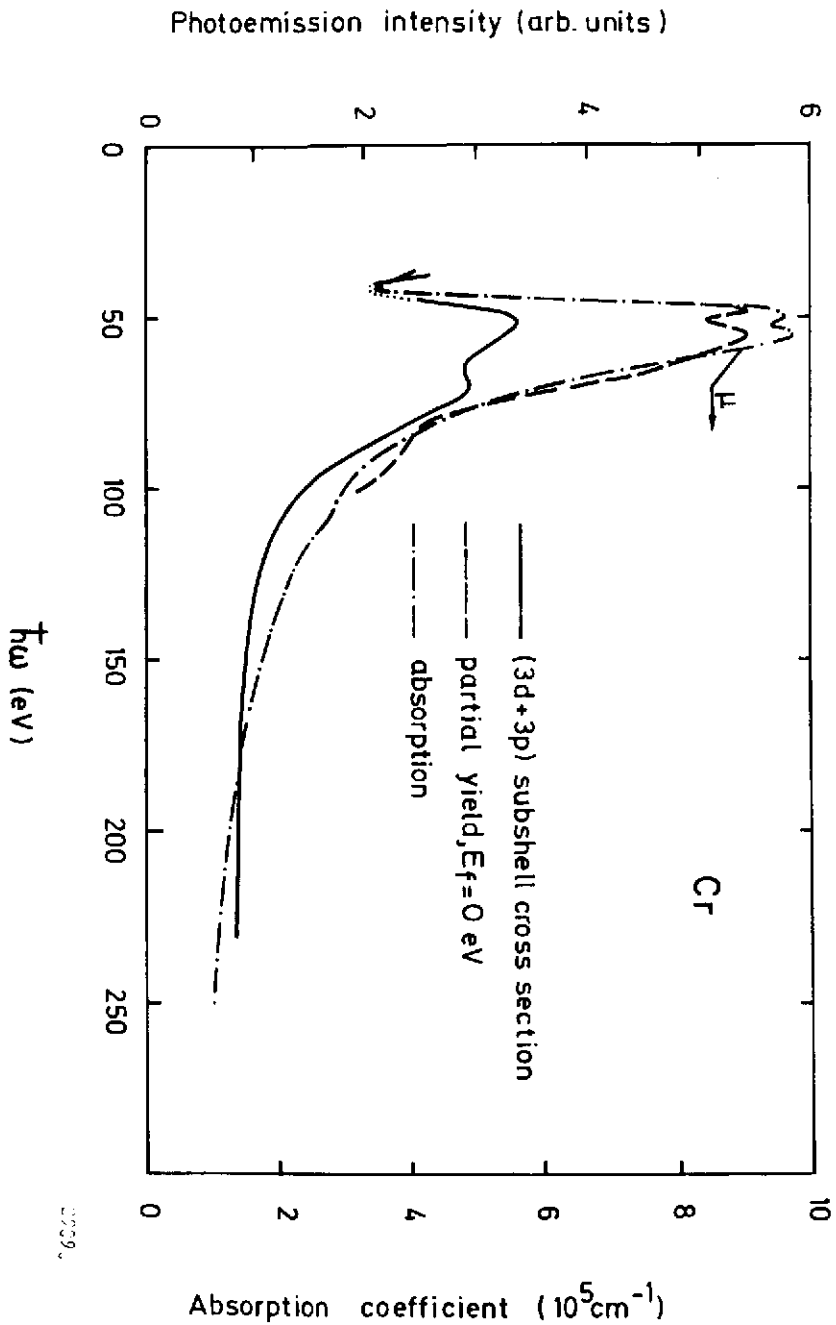
Photoemission intensity (arb. units)
0
2
4
6
0
50
100
150
200
250
ħω (eV)
(3d+3p) subshell cross section
partial yield, E_f=0 eV
absorption
Cr
0
2
4
6
8
10
Absorption coefficient (10^5 cm^-1)

Fig. 3

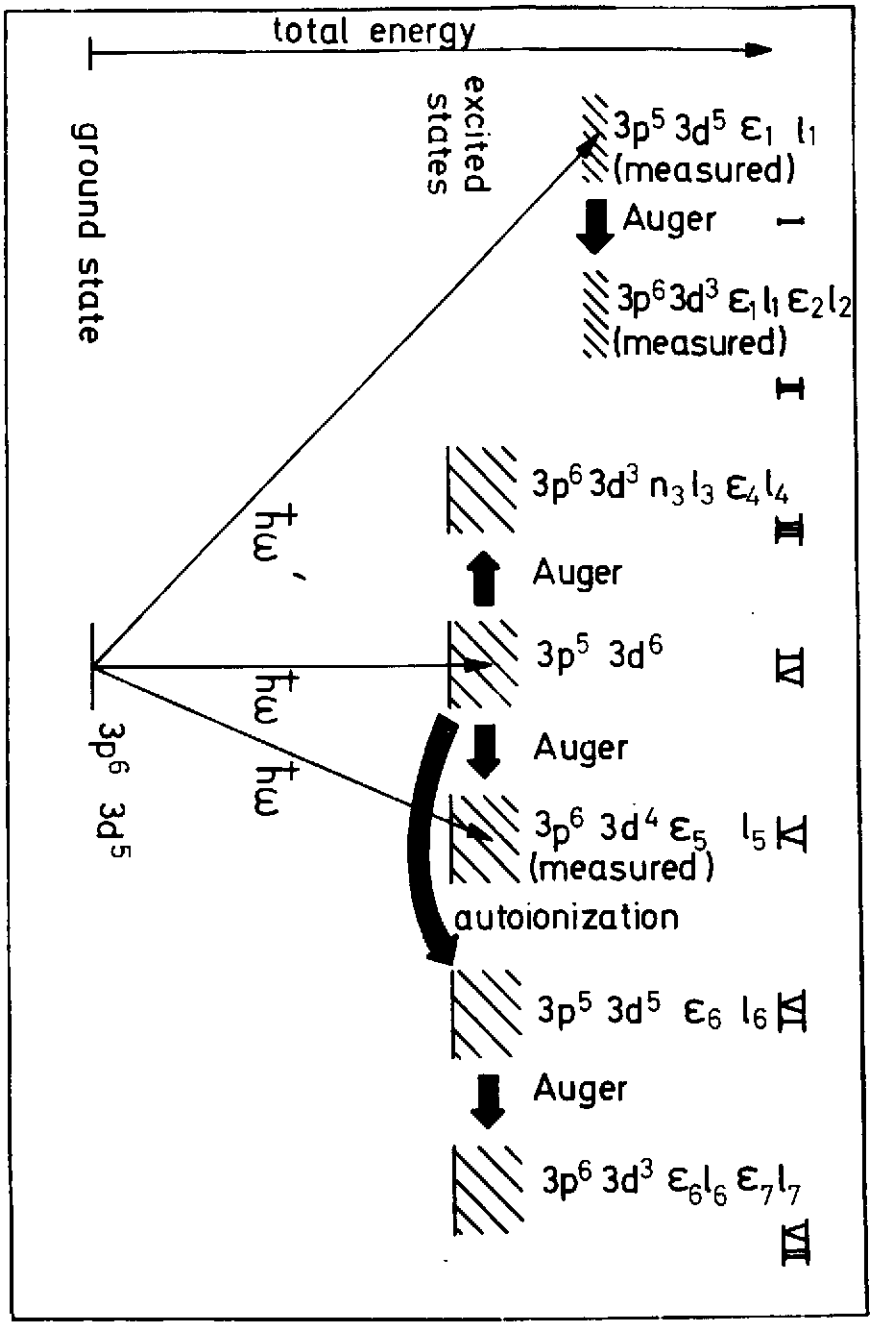
total energy
ground state
excited states
3p^6 3d^5
ħω
ħω'
ħω
3p^5 3d^5 ε_1 l_1
(measured)
Auger
I
3p^6 3d^3 ε_1 l_1 ε_2 l_2
(measured)
II
3p^6 3d^3 n_3 l_3 ε_4 l_4
III
Auger
3p^5 3d^6
IV
Auger
3p^6 3d^4 ε_5 l_5
(measured)
V
autoionization
3p^5 3d^5 ε_6 l_6
VI
Auger
3p^6 3d^3 ε_6 l_6 ε_7 l_7
VII

Fig. 4